Journal of Sound and Vibration 329 (2010) 1673–1685

Contents lists available at ScienceDirect

Journal of Sound and Vibration

journal homepage: www.elsevier.com/locate/jsvi

Modeling of wall pressure fluctuations for finite element structural analysis

Chinsuk Hong [a,*], Ku-Kyun Shin [b]

[a] School of Digital Mechanics, Ulsan College, 148, Deahakro, Mugeodong, Nam-gu, Ulsan 680-749, Republic of Korea
[b] Agency for Defense Development, P.O. Box 18, Chinhae Post Office, Gyeongnam 645-600, Republic of Korea

ARTICLE INFO

Article history:
Received 16 December 2008
Received in revised form
15 October 2009
Accepted 23 November 2009
Handling Editor: L.G. Tham
Available online 29 December 2009

ABSTRACT

This paper investigates a modeling technique of wall pressure fluctuations (WPF) due to turbulent boundary layer flows on a surface for finite element structural analysis. This study is motivated by critical issues of structural vibrations due to turbulent WPF over the surface of a body. The WPFs are characterized with random behavior in time and space. The temporal and spatial random behavior of the WPFs is mathematically expressed in the form of the auto- and cross-power spectral density functions (PSDF) in the frequency domain (e.g., Corcos Model). For finite element modeling of the random distributed fluctuations, the cross-PSDF is properly modeled over the finite element structural mesh. The quality of modeling of the cross-PSDF is directly affected by the structural mesh size. We first examine the maximum mesh size required for reliable finite element analysis. The reliability of the FEA results is confirmed by the theoretical results. It is found that the maximum mesh size should be determined under consideration of the spatial distribution of the cross-PSDF in addition to the representation of dynamic behavior of the structure in the frequency range of interest. It is also recognized that the requirement of the maximum mesh size is unrealistic in many practical cases. We then investigate practical modeling schemes under a realistic mesh size condition. We found that the WPF can be modeled without the exact consideration of cross-correlation if the power due to the wall pressure fluctuation can be properly compensated. This is owing to the feature of decreasing the cross-correlation of WPFs at high frequencies and the fact that the WPF does weakly couple into the structural modes at high wavenumbers such that $2\pi f/U_c < k_{\max}$. The wall pressure fluctuations can therefore be modeled as uncorrelated loadings with power compensations.

1. Introduction

Due to the viscosity, fluid flow over a surface forms a boundary layer [1]. The movement of fluid particles then becomes complicated, and this complicated flow produces wall pressure fluctuations (WPF). The wall pressure fluctuations under a fully developed turbulent boundary layer (TBL) flow were first measured on a flat plate with no pressure gradient [2]. Since then, wall pressure fluctuations have been thoroughly researched theoretically [3] and experimentally [4,5]. Since the 1960s, the characteristics of WPF under turbulent boundary layer have also been mathematically identified and modeled.

* Corresponding author. Tel.: +82 52 279 3134; fax: +82 52 279 3137.
E-mail addresses: cshong@uc.ac.kr, csh@isvr.soton.ac.uk (C. Hong), kkshon@add.re.kr (K.-K. Shin).

0022-460X/$ - see front matter © 2009 Elsevier Ltd. All rights reserved.
doi:10.1016/j.jsv.2009.11.026

Mathematical models of WPF under TBL on an infinite plane surface having no pressure gradient are presented [6–8]. Wall pressure fluctuations act as excitation forces on flexible structures that lead to structural vibrations.

The flow-induced vibration due to the wall pressure fluctuations is sometimes a critical issue. For aircrafts and space vehicles, for instance, the fuselage suffers from strong vibrations due to wall pressure fluctuations at high speeds. The strong vibrations increases the noise level in the cabin and this increases passengers' discomfort. The strong vibration at high speed flight is due to a physical phenomenon called wavenumber-matching when the wavenumber of the wall pressure fluctuations coincides with that of the structural response [4,5]. For underwater vehicles, the WPF on the wet surface can vibrate the ship's hull, and then generate radiated noise. For the SONARs of underwater vehicles including ships, submarines and torpedoes, the WPF on the acoustic window of the array of sensors generates pseudo-sound and increases the self-noise of the SONAR. This self-noise directly affects the SONAR detection performance.

For these reasons, the structural response due to the WPF should be considered in controlling noise and vibrations. In order to reduce the unwanted noise and vibration due to WPF, turbulent boundary layer flow and turbulent intensity should be alleviated by optimizing the lines of a hull. However, noise control by flow optimization is limited due to other requirements. Hence, typical noise and vibration control techniques can be applied to structures; these techniques include the use of damping materials, absorbing materials, decouplers, etc. Prior to applying these noise control techniques to structures the structural dynamics of the vehicles should be characterized.

Structural vibration and radiated noise due to WPF under turbulent boundary layer flows have been investigated experimentally and theoretically. The response of infinite plates to WPF was studied [9,10]. Furthermore, the response of finite plates to WPF was investigated [11–15]. The response of water-loaded simply supported plates to WPF for homogeneous boundary layer flow was also investigated [16]. Theoretical solutions, for either infinite plates or simply supported plates, are obtained by the time–space Fourier transform of impulse responses and wall pressure fluctuations. Since the response and the WPF over the surface can be transformed into wavenumber-frequency functions, the response to WPF can be obtained theoretically. For complicated structures that are no longer assumed to be plate structures, however, the theoretical approach becomes no longer applicable and so, a numerical approach, e.g., finite element method (FEM), is employed.

In FEM, the structures are discretized with meshes composed of nodes and elements. The size of the mesh is determined by the two requirements that are used to properly represent the spatial distribution of the input and the response within the frequency range of interest. Firstly, for the representation of the response, the size of the mesh to model the structure should be small enough to depict the spatial behavior of structural response within the frequencies of interest. This mesh size is determined iteratively by modal analysis with reducing mesh size until the highest order natural mode to be superposed is well represented. The corresponding highest natural frequency is greater than double the maximum frequency of interest. Secondly, for spatially distributed input forces, the size of the mesh should be also small enough to represent the spatial variation of the forces. Structural excitation forces due to WPF are spatially distributed over the surface of the structure. The excitation is characterized as random in time as well as in space. The feature of this excitation can be modeled by the cross-correlation functions. The wavenumber spectrum of the cross-correlation of WPF has the highest power at the convective wavenumber. The cross-correlation functions, at least, at the double of the convective wavenumber should be well represented over the discretized mesh.

The mesh required for the spatial variation of WPF is too small in most cases to practically model the structure for finite element analysis. This paper focuses on the modeling schemes for WPF over a discretized surface for finite element analysis. In Section 2, for a simple beam structure, the mathematical formula of the exact solution and a finite element analysis are presented. Finite element modeling of the wall pressure fluctuations due to turbulent boundary layer flows is demonstrated for three different methods in Section 3. Conclusions from this study are summarized in Section 4.

2. Theory

2.1. Mathematical models of WPF in turbulent boundary layers

Wall pressure fluctuations generated on the surface of structures due to the complicated movement of fluid particles in turbulent boundary layers become a source of structural vibration. A mathematical source model of WPF is required to calculate the vibrational response of a structure due to WPF. Many practical sources, machinery for example, can be modeled by descriptions of the deterministic forces at mounting locations. The deterministic forces are expressed by magnitudes and phases. On the other hand, wall pressure fluctuations are random in time and space. These random sources distributed over a surface should be expressed by random variables, e.g., power spectral density functions (PSDF). The randomness of WPF is caused by the physical behavior of eddies in the turbulent boundary layer on the surface of a structure. Of the eddies, the larger ones become smaller ones, which are in turn divided into much smaller ones that are eventually dissipated while convecting downstream. Due to the eddies flowing downstream, the pressure at a point affects the pressure fluctuation at neighboring points in the form of random processes in time and space. Therefore, WPF can be modeled in terms of auto- and cross-spectral density functions.

Of the models [6–8], the Corcos model is used in this paper, which is relatively easy to handle and is reliable. The Corcos model is given in the form of the cross-power spectral density function, $C_{pq}(\gamma_x, \gamma_y; \omega)$, as follows:

$$C_{pq}(\gamma_x, \gamma_y; \omega) = C_{pp}(\omega) A(\omega\gamma_x/U_c) B(\omega\gamma_y/U_c) e^{-j(\omega\gamma_x/U_c)}, \tag{1}$$

where $C_{pp}(\omega)$ is the auto-power spectral density function, U_c is the convective velocity of the eddies in the turbulent boundary layer. γ_x and γ_y are the coordinates of point q in the local coordinate system with the origin at the point p whose x-axis coincide with the flow direction. ω is angular frequency and the functions $A(\omega\gamma_x/U_c)$ and $B(\omega\gamma_y/U_c)$ are called *Corcos functions* representing cross-correlation along the flow direction and its normal direction, respectively. The Corcos functions are represented in the form of

$$A = \exp(-\alpha|\omega\gamma_x/U_c|) \tag{2}$$

and

$$B = \exp(-\beta|\omega\gamma_y/U_c|), \tag{3}$$

where α and β can be set to 0.1 and 0.7 [7], respectively, for smooth plates. The spatial Fourier transform of Eq. (1) leads to the wavenumber-frequency spectrum of WPF as

$$C_{pq}(k_x, k_y; \omega) = C_{pp}(\omega) \cdot \frac{\alpha k_c/\pi}{(k_x - k_c)^2 + (\alpha k_c)^2} \cdot \frac{\beta k_c/\pi}{k_y^2 + (\beta k_c)^2}, \tag{4}$$

where $k_c = \omega/U_c$ is the convective wavenumber. Note that a one-dimensional model of WPF can be obtained, if necessary for simplicity as shown in Fig. 1, by rewriting Eqs. (1)–(4) for $\gamma_y = 0$, $\beta = 0$ and $k_y = 0$. Fig. 2 shows the wavenumber

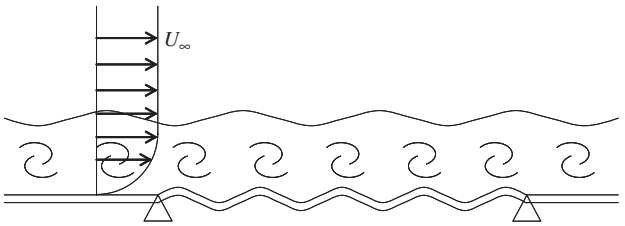

Fig. 1. A simply supported beam subjected to turbulent wall pressure fluctuations.

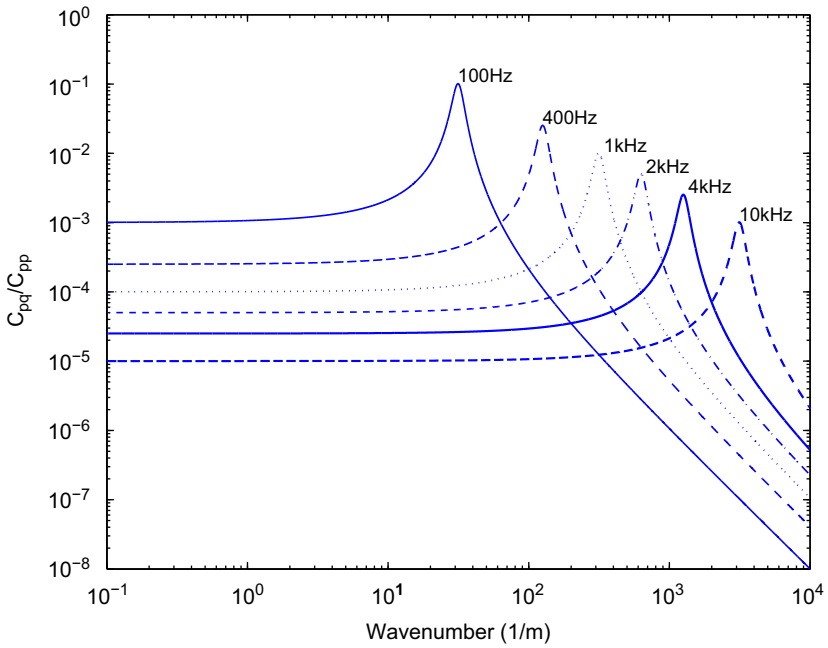

Fig. 2. Wavenumber spectra at several frequencies of 100 Hz (solid line), 400 Hz (dashed), 1 kHz (dotted line), 2 kHz (dash-dotted line), 4 kHz (thick solid line) and 10 kHz (thick dashed line) when $U_c = 20$ m/s.

spectrum of WPF at $U_c = 20\,\mathrm{m/s}$ for several frequencies of 100 Hz, 1, 2, 4 and 10 kHz when $U_c = 20\,\mathrm{m/s}$. It should be pointed out that the spectra have their maxima at the convective wavenumbers.

2.2. Exact solution of beam's response to WPF

The simplest example of structures subjected to WPF is a plate because its flow field, which generates the WPF, is at least two dimensional. For simplicity, however, the TBL flow on a beam structure is considered under the assumption that fluid flows along the beam length and the flow characteristics normal to the flow direction is neglected. Fig. 1 shows a homogeneous boundary layer flow on a simply support elastic beam of length L between infinite baffles. The transverse vibration of the beam is governed by

$$EI(1+j\eta)\frac{\partial^4 u(x,t)}{\partial x^4} + m\frac{\partial^2 u(x,t)}{\partial t^2} = p_t(x,t), \tag{5}$$

where EI is the bending rigidity, η the structural damping coefficient, m is the mass per unit length and $p_t(x,t)$ is the WPF due to the turbulent boundary layer flow.

The response at x to the pressure at x', i.e., $p_t(x,t) = \delta(x-x')e^{j\omega t}$, can be obtained by the modal superposition method

$$H(x,x';\omega) = \frac{1}{m}\sum_{n=1}^{\infty}\frac{\phi_n(x)\phi_n(x')}{(\omega_n^2-\omega^2)+j\eta\omega_n^2}, \tag{6}$$

where ω is the excitation frequency, and ω_n and $\phi_n(x)$ are the nth natural frequency and the corresponding natural mode shape function, respectively, which can be written for simply supported beams as

$$\phi_n(x) = \sqrt{2}\sin\frac{n\pi}{L}x \tag{7}$$

and

$$\omega_n = \sqrt{\frac{EI}{m}}\left(\frac{n\pi}{L}\right)^2. \tag{8}$$

Since the excitation force due to WPF in turbulent boundary layer flows is random in space, it can only be expressed in the form of the cross-power spectral density function as shown in Eq. (1). Response to a random excitation should be written in the form of a cross-power spectral density function. The cross-power spectral density function of a displacement at x can be obtained by

$$S_{uu}(x,\xi;\omega) = \int_0^L\int_0^L C_{pq}(\xi',\omega)H(x,x';-\omega)H(x+\xi,x'+\xi';\omega)\,\mathrm{d}x'\,\mathrm{d}\xi'. \tag{9}$$

From Eq. (9), by letting $\xi = 0$, the auto-power spectral density of the displacement at x, $S_{uu}(x,\omega)$, can be obtained. The auto-power spectral density function can be expressed in the wavenumber-frequency domain as

$$S_{uu}(k,\omega) = \frac{1}{(2\pi)^2}\sum_{n=1}^{\infty}\left[\phi_n^2(x)|h_n(\omega)|^2\int_{\infty}C_{pq}(k,\omega)|\Phi_n(k_x)|^2\,\mathrm{d}k_x\right], \tag{10}$$

where

$$h_n(\omega) = \frac{1}{m}\frac{1}{(\omega_n^2-\omega^2)+j\eta\omega_n^2}, \tag{11}$$

and $\Phi_n(k_x),\ n = 1,2,\ldots$ are the spatial Fourier transforms of the mode shape functions, $\phi_n(x)$.

2.3. Finite element solution of beam's response to WPF

In this section, a general procedure for calculating the vibration responses of linear deterministic systems to random excitations due to WPF is briefly introduced. The random excitations due to WPF are expressed by the cross-power spectral density function given by Eq. (1). The responses of deterministic structures to the random excitations are also expressed in the form of spectral density functions, correlation functions and root mean square (RMS) values of displacements, velocities, accelerations, stresses, strains, etc. The relationship between the random excitation and the response functions is hence derived in terms of the transfer functions of the structures. The displacement response at a node j, $u_j(\omega)$, to correlated random excitations, $F_p(\omega),\ p = a,b,c,\ldots$ as shown in Fig. 3, can be written as

$$u_j(\omega) = [H_{ja}\ H_{jb}\ H_{jc}\cdots H_{jn}]\begin{Bmatrix}F_a(\omega)\\F_b(\omega)\\\vdots\\F_n(\omega)\end{Bmatrix}, \tag{12}$$

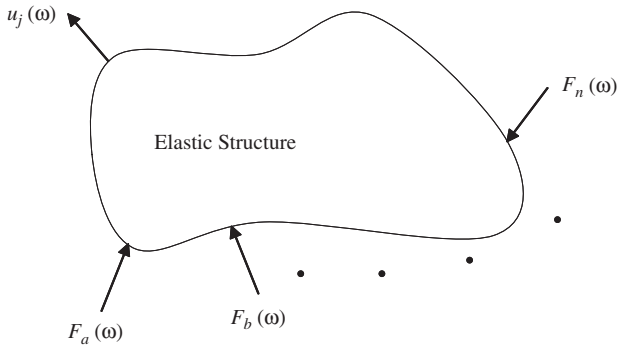

Fig. 3. An elastic structure subjected to random forces.

where $H_{ja}(\omega)$ is the displacement response at a node j to a unit excitation at a node a. The auto-power spectral density function of the response $u_j(\omega)$ can be expressed as

$$S_{u_j u_j}(\omega) = T\langle u_j(\omega) u_j^*(\omega)\rangle, \tag{13}$$

where T is the averaging time, $\langle\ \rangle$ denotes time-averaging and the superscript $*$ denotes the complex conjugate. Substituting Eq. (12) into Eq. (13), the auto-power spectral density function of the response can be therefore obtained as

$$S_{u_j u_j}(\omega) = \mathbf{H}_j(\omega)\mathbf{S}_{\mathrm{IN}}(\omega)\mathbf{H}_j^{\mathrm{H}}(\omega), \tag{14}$$

where the superscript H denotes the Hermitian transpose,

$$\mathbf{H}_j(\omega) = [H_{ja}\ \ H_{jb}\ \ H_{jc}\cdots H_{jn}], \tag{15}$$

and the power spectral density matrix of the excitations is written as

$$\mathbf{S}_{\mathrm{IN}}(\omega) = \begin{bmatrix} S_{aa}(\omega) & S_{ab}(\omega) & \cdots & S_{an}(\omega) \\ S_{ba}(\omega) & S_{bb}(\omega) & \cdots & S_{bn}(\omega) \\ \vdots & \vdots & \ddots & \vdots \\ S_{na}(\omega) & S_{nb}(\omega) & \cdots & S_{nn}(\omega) \end{bmatrix}. \tag{16}$$

$S_{pq}(\omega)$ in Eq. (16) is the cross-power spectral density function which can be estimated by $T\langle F_p(\omega)F_q^*(\omega)\rangle$, holding the relationship, $S_{pq}(\omega) = S_{qp}^*(\omega)$. Note that

$$S_{pq}(\omega) = A_p A_q C_{pq}(\omega), \tag{17}$$

where A_p and A_q are the effective areas of the nodal points, p and q, respectively.

In finite element analysis, the transfer function matrix given in Eq. (15) is first constituted by calculating the transfer function repeatedly for each excitation point, and the power spectral density function of the response, Eq. (14), is then estimated by utilizing the input matrix of the power spectral density function of the excitation, $\mathbf{S}_{\mathrm{IN}}(\omega)$. Many commercial FE softwares, e.g., MSC.NASTRAN and ANSYS, have the capability for this procedure. Note that the input matrix, Eq. (16), should be prepared by collecting the function values of Eq. (1) over the finite element mesh at each frequency. In the next section, we investigate several approaches for the finite element modeling of WPF in detail.

3. Finite element modeling of WPF

3.1. Fully correlated model

Determination of the maximum mesh size of a structural finite element model is the first step toward a reliable analysis. To represent the requirement for the maximum mesh size, adopting the Nyquist sampling theorem for space and wavenumber, we introduce the sampling wavenumber,

$$k_s = 2\pi/\Delta x, \tag{18}$$

for the maximum mesh size, Δx. The responses and excitations can then completely depicted with spatial variation up to the maximum wavenumber given by

$$k_{\max} = k_s/2. \tag{19}$$

Two requirements are applied to determine the maximum mesh size. (1) The maximum mesh size should be determined based on the requirement that the mode shape function is well expressed, whose the natural frequency is higher than

double the maximum frequency of interest. This requirement can be written as

$$k_{\max}^{(r)} \geq 2k_{\text{mode}}, \tag{20}$$

where k_{mode} is the wavenumber of the highest order mode to be superposed. (2) The maximum mesh size should, in addition, be determined by the requirement that the excitation forces are well depicted over a discretized mesh when they are distributed over the structure with a spatial variation. For modeling of the WPF, the cross-power spectral density function given by Eq. (1) should be modeled over the discretized mesh. The cross-PSDF is the cross-correlation function multiplied by the auto-PSDF. Hence, the cross-correlation function should be depicted over the discretized mesh. Based on Eq. (4), the cross-PSDF has a maximum at $k_x = k_c$, for a one-dimensional case, where $k_c = \omega/U_c$. Therefore, the maximum mesh size for the WPF can be obtained from the condition

$$k_{\max}^{(e)} \geq 2k_{c,\max}, \tag{21}$$

where $k_{c,\max}$ is the convective wavenumber at the maximum frequency of interest, $\omega_{\max}$, i.e.,

$$k_{c,\max} = \omega_{\max}/U_c. \tag{22}$$

Combining the two requirements for the discretization of the structure, the maximum mesh size, Δx, can be determined from

$$k_{\max} \geq \max(k_{\max}^{(r)}, k_{\max}^{(e)}). \tag{23}$$

Therefore, for a finite element structural vibration analysis under excitations due to WPF up to $\omega_{\max}$, the maximum mesh size, Δx, can be determined. Using the relationships from Eqs. (18) to (21) and the requirement for the mesh size given by Eq. (23), the maximum mesh size is

$$\Delta x = \frac{\pi}{k_{\max}}. \tag{24}$$

The beam structure shown in Fig. 1 is again considered. The beam's geometry and material properties are listed in Table 1. The vibratory response to WPF is calculated using the finite element method. The WPF is given by Eq. (1), which is referred to as the Corcos model. The finite element mesh of the beam structure is obtained using the maximum mesh size. Then, the power spectral density matrix of Eq. (16) is developed for the finite element mesh by substituting the coordinates of the nodal points into Eq. (1). The vibration response can be calculated using Eq. (14). The result of this finite element analysis (FEA) can be thus compared with the exact solution obtained in Section 2.2. If the finite element mesh is satisfied with the requirement given by Eq. (24), the FEA results should be almost the same as the exact solution. The maximum frequency of interest is considered to be 4 kHz in this paper. The beam is discretized based on the requirement stated in Eq. (24). Note that the maximum mesh size is affected by the convection velocity since the spatial variation of the wall pressure fluctuation described by the cross-correlation function as in Eq. (4) depends on the convection velocity. The convection velocity considered here was 200 m/s.

In order to determine the maximum mesh size, we first extracted the natural frequencies and mode shapes of the beam and obtained the maximum modal wavenumber in the frequency range of interest, $k_{\text{mode}} = 10\pi$ in this case, so that $k_{\max}^{(r)} \geq 20\pi$ from Eq. (20). Then, the maximum convective wavenumber, denoted by $k_{c,\max}$ in this case, was considered to be 40π from Eq. (22) with $\omega_{\max} = 2\pi \times 4000$ and $U_c = 200$ m/s. According to the requirement for the maximum mesh size stated in Eq. (24), the maximum mesh size was determined to be 0.01 m with $k_{\max} = 100\pi$. Fig. 4 shows the wavenumber spectra of WPF at $U_c = 200$ m/s for several frequencies of 100 Hz, 1, 2, 4 and 10 kHz when $U_c = 200$ m/s. The comparison of the wavenumber for the maximum mesh size with the convective wavenumber at the maximum frequency of interest showed that the selected mesh size was suitable for the analysis under the excitation (WPF) and the given frequency of interest.

Fig. 5 shows the representation of the cross-correlation functions at 4 kHz (real part: faint solid, imaginary part: dashed line) and 400 Hz (real part: thick solid, imaginary part: thick dashed line) when $U_c = 200$ m/s. Since the values of the cross-correlation functions over the mesh are defined only at the nodal points, Fig. 5 shows how well the mesh can depict the spatial variation of the cross-correlation functions for a reliable analysis. It can be seen that the quality of the representation of the cross-correlation become worse as the frequency increases. The mesh for the condition in this example can be recognized to be acceptable. The selected maximum mesh size, 0.01 m in this example, can depict the

Table 1
Mechanical properties and geometric data of beams.

Parameters	Symbol	Unit	Values
Length	L	m	1
Moment of inertia	I	m^4	3×10^{-8}
Density	ρ	kg/m^3	2650
Young's modulus	E	GPa	71
Loss factor	η	–	0.02
Poisson ratio	v	–	0.3

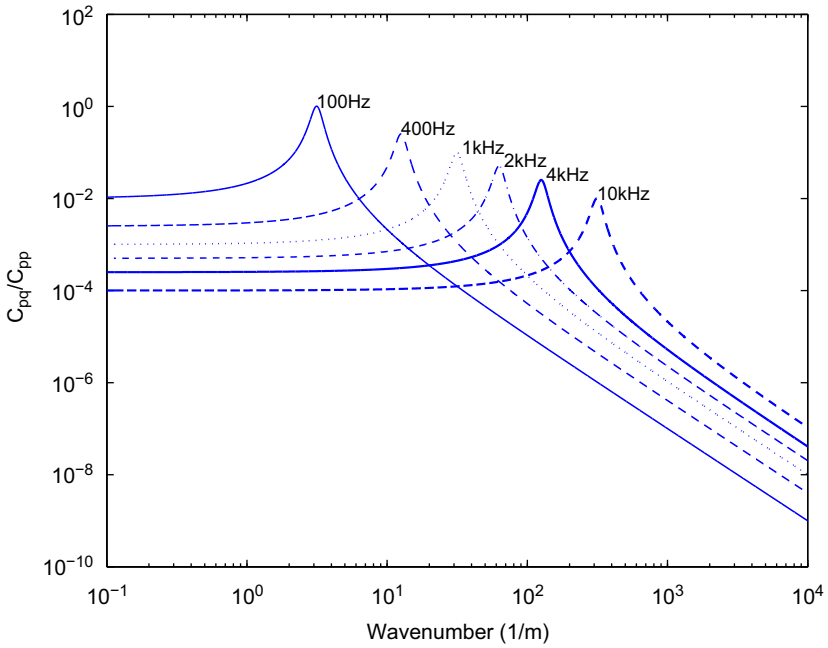

Fig. 4. Wavenumber spectra at several frequencies of 100 Hz (solid line), 400 Hz (dashed), 1 kHz (dotted line), 2 kHz (dash-dotted line), 4 kHz (thick solid line) and 10 kHz (thick dashed line) when $U_c = 200$ m/s.

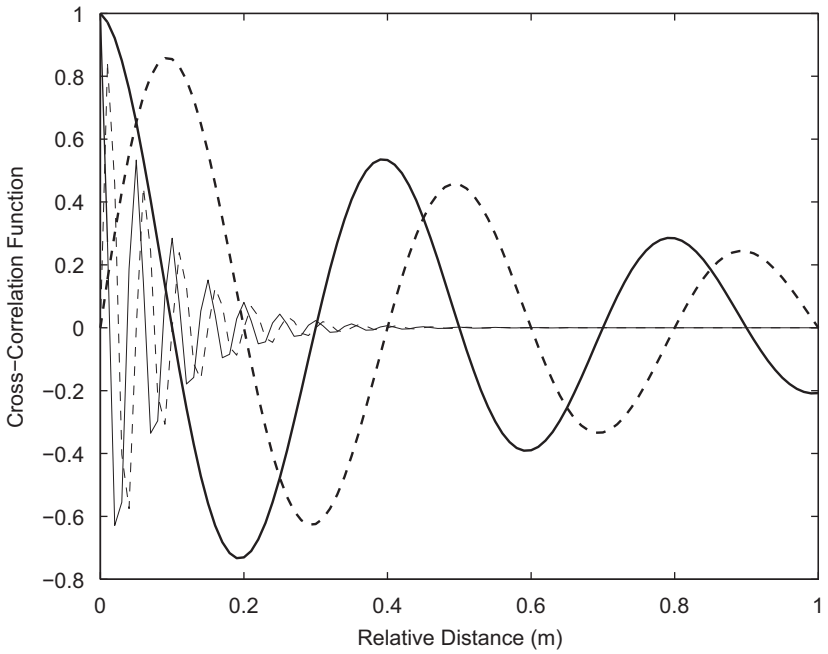

Fig. 5. Representation of the cross-correlation functions at 4 kHz (real part: faint solid, imaginary part: dashed line) and 400 Hz (real part: thick solid, imaginary part: thick dashed line) when $U_c = 200$ m/s.

spatial distribution of the cross-correlation at 4 kHz, the maximum frequency of interest. Fig. 6 shows the displacement power spectral density function at the center point of the beam calculated by the theory presented in Section 2.2 and by FEM presented in Section 2.3. They agreed well at higher frequencies but they start to show a difference as the frequency decreases at low frequencies. The deviations at the low frequency range are caused by the correlation terms due to the upstream disturbances, which are not modeled. In fact, the upstream disturbances over the baffle affect the disturbances over the elastic structure since the disturbance at lower frequencies have a longer correlation length, as shown in Fig. 5. To

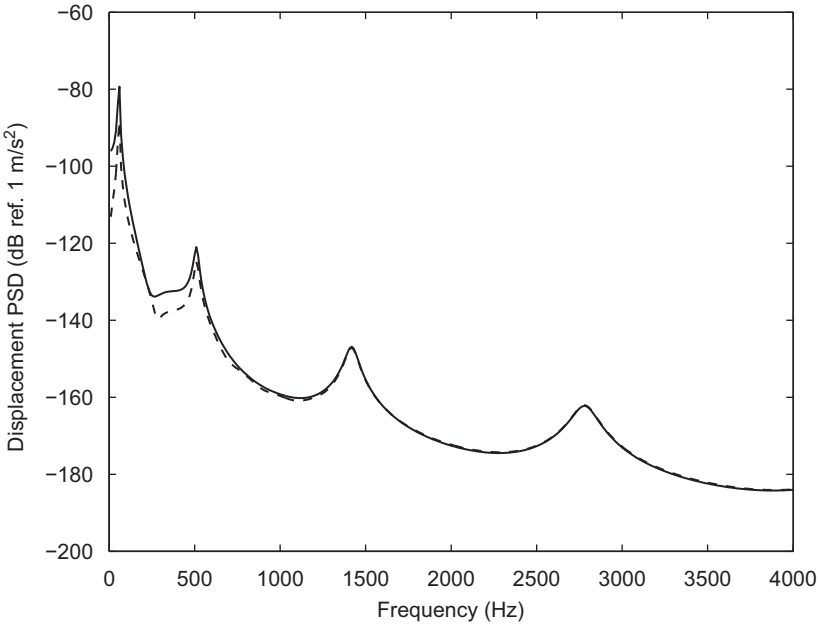

Fig. 6. Comparison of the displacement power spectral density function obtained by FEM (solid line) with the exact solution (dashed line) at $x = 0.5$ m of the beam subjected to the wall pressure fluctuation when $U_c = 200$ m/s.

take into account the long correlation length at a lower frequency, we should model a long dummy structure upstream to perfectly model the upstream effect. The modeling of the upstream disturbance effect is, however, out of the scope of this paper.

3.2. Limitations of modeling fully correlated loading

We can obtain a good numerical solution using the finite element analysis, provided that the structures are modeled with an adequate mesh size satisfying the requirement given by Eq. (24) and the dummy structure having enough length to reflect the upstream effect. However, it could be, in practice, impossible for engineers to accept both requirements above, particularly for low upstream speeds. When the upstream speed is such a low speed that $k_{c,\max} \gg k_{\mathrm{mode}}$, the requirement for the maximum mesh size is affected only by Eq. (21). This means that the structure should be discretized with very small meshes due to the spatial variation of WPF at a high wavenumber although the frequency range of interest is relatively low. When the accuracy of the response at low frequencies needs to be improved, dummy meshes are required to take into account the upstream effect on the flexible structure. The length of the dummy mesh is sometimes too long to model. For the example solved in Section 2.3, the upstream velocity is 200 m/s so the length of the dummy structure to achieve the perfect correlation effect is about 1 m. As the frequency limit required to pertain the exact solution decreases, the required length of the dummy structure increases at the same rate. Furthermore, the required length of the dummy structure also increases with decreasing upstream velocity. For instance, the dummy structure length should be about 40 m to perfectly reflect the upstream effect at 100 Hz.

According to the exact solution given by Eq. (10), the high power around the convective wavenumber ($k_{c,\max} = \omega/U_c$) does not directly affect the response of the structure when $k_c \gg k_{\mathrm{mode}}$. This means that the excitation due to WPF does not couple into the modes in the frequency range of interest. With respect to mesh size, thus, the maximum mesh size may be obtained based on the requirement for only depicting the response of the structure at the highest frequency of interest. It might be misunderstood that the accuracy of the finite element analysis is not improved by decreasing the mesh size to satisfy the requirement $k_{\max} > k_{c,\max}$. Note that, however, the lack of meshes leads to errors in the predicted response due to spatial aliasing.

To find the characteristics of the errors due to the lack of meshes for depicting the WPF, we calculated the response at 20 m/s with a lager mesh size and compared it with the exact solution given by Eq. (10). The larger mesh did not meet the requirement for depicting WPF but did meet the requirement for depicting the response at the maximum frequency of interest. With this larger mesh, we modeled the WPF in two ways: fully correlated loading denoted by $C_{pq}(\omega)$ in Eq. (1) and uncorrelated loading denoted by $C_{pp}(\omega)$, assuming that $C_{pp}(\omega) = 1$ at each frequency in this study. Fig. 7 shows the displacement power spectral density functions at $x = 0.5L$ for an upstream speed of 20 m/s: the exact solution and the responses to either the fully correlated loading or uncorrelated loading. Note that the fully correlated loading is modeled over the discretized surface with a coarse mesh. Fig. 8 shows that the mesh can depict well the correlation function at the

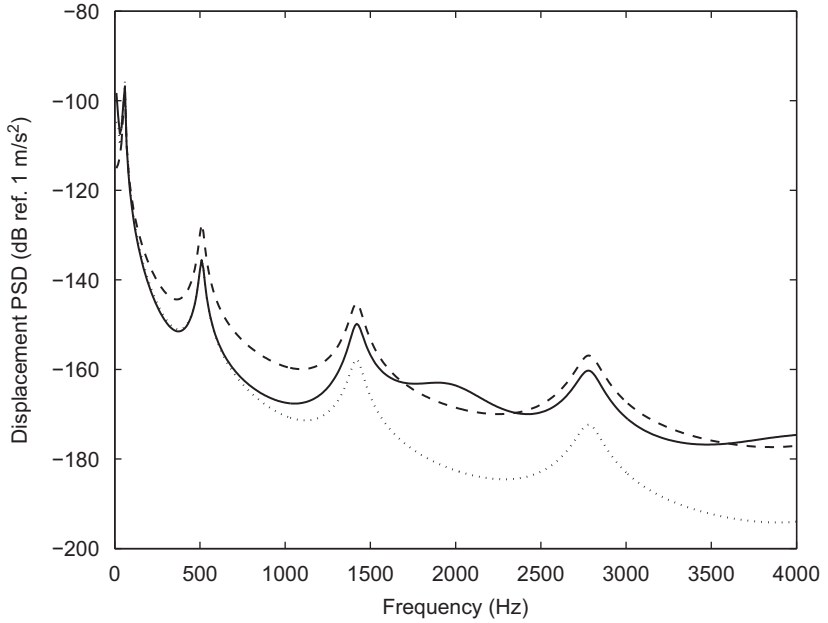

Fig. 7. Effects of the coarse mesh on the displacement power spectral density functions at $x = 0.5$ m, subjected to WPF modeled by the fully correlated power over the coarse mesh (solid line), by the uncorrelated power (dot-dashed line) and by theory (dotted line).

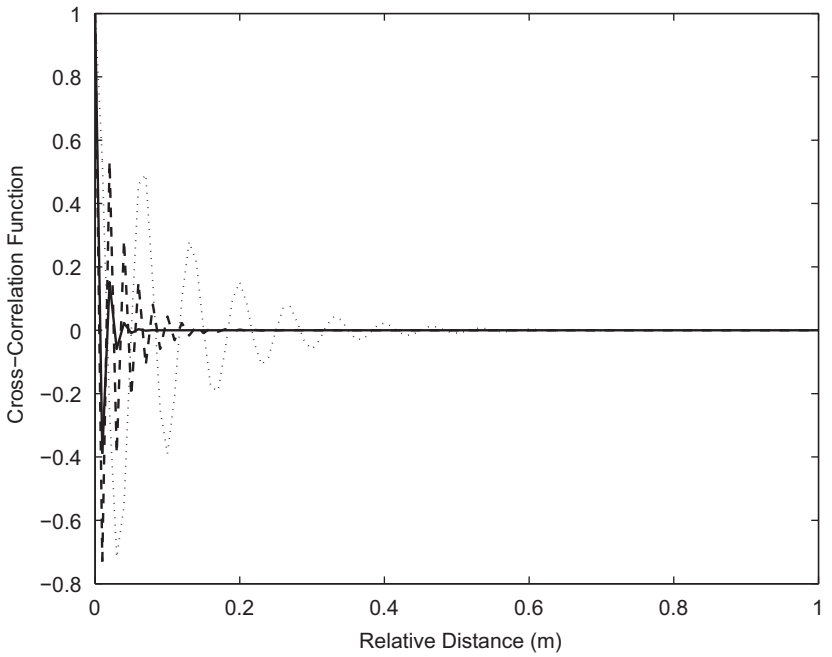

Fig. 8. Representation of the cross-correlation functions over the coarse mesh at 3 kHz (solid), 1 kHz (dashed line) and 300 Hz (dotted line) when $U_c = 20$ m/s.

low frequencies but the quality of the depiction of the correlation on the mesh decreases as the frequency increases. The response to the fully correlated loading well agrees with the exact solution at the low frequencies below 700 Hz, but it approaches the response to the uncorrelated loading at high frequencies greater than 700 Hz. The deviation from the exact solution at the high frequencies is due to the loss of the spatial correlation over the coarse discretization of the surface. The coarse mesh leads to the aliasing effect in the sampled spatially distributed correlation function. We then considered compensations of the loss of the spatial correlation due to the lack of meshes. Two approaches were attempted:

compensation of the aliased power (filtered power model) and theoretical modeling of the correlation inside elements (compensated uncorrelated model).

3.3. Filtered power model

Due to the lack of meshes, the correlation over the coarse meshes leads to the aliasing in the spatially correlated power to be input to the structure. The aliasing causes the sampled input power to be overlapped in the wavenumber spectrum shown in Fig. 2 with respect to $k_{\max}$. There is no way, in principle, to tell the exact correlation function from modeling it over these coarse meshes. However, the feature of a typical wavenumber spectrum shown in Fig. 2 showing only one peak value at the convective wavenumber gives a possibility of the compensation. We can estimate the genuine power input excluding the aliased power by integrating the wavenumber spectrum from $-k_{\max}$ to $k_{\max}$ at each frequency. We reflected the compensation into the auto-power spectral density function. Fig. 9 shows the compensated input power spectral density function (solid line) compared with the original auto-power spectral density function (dashed line) which is 0 dB in this example. Since the spatial correlation is well represented at low frequencies, a small compensation is required. On the other hand, the compensation needs to be increased at higher frequencies where the aliasing seriously occurs.

The vibratory response of the beam to WPF is calculated when $U_c = 20\,\mathrm{m/s}$ using FEA. The input power of the WPF is compensated by the filtered power model (solid line in Fig. 9). Fig. 10 shows the calculated displacement PSDF at $x = 0.5L$ of the beam (solid). It is compared with the theoretical displacement PSDF (thick solid) given by Eq. (10). The deviation shown in Fig. 7 is now alleviated due to the compensation. We can then obtain a reliable solution even with a coarse mesh owing to the compensation. Note that, however, this scheme still requires to model the cross-correlation terms for FEA, which is quite complicated. We attempted to model WPF for FEA without the cross-correlation terms. The dashed line in Fig. 10 denotes the response to the uncorrelated filtered power compensation. This shows a good agreement with the exact solution at high frequencies. Since the cross-correlation terms between two spatial points are decreased as the frequency increases, the uncorrelated loading model with this compensation scheme gives a reliable solution at high frequencies. In the subsequent section, we discover this characteristics mathematically and suggest a practical compensation scheme.

3.4. Compensated uncorrelated model

Another compensation procedure is presented mathematically. Consider the frequency where the correlation completely lost due to the coarse mesh. Under this circumstance, the input PSDFs are completely uncorrelated. Only the diagonal terms of the matrix, $\mathbf{S}_{\mathrm{IN}}(\omega)$, remain. The displacement PSDF, Eq. (13), can be therefore rewritten as

$$S_{u_j u_j}(\omega) = \sum_{a=1}^{N} H_{aj} S_{aa} H_{aj}^{*}. \tag{25}$$

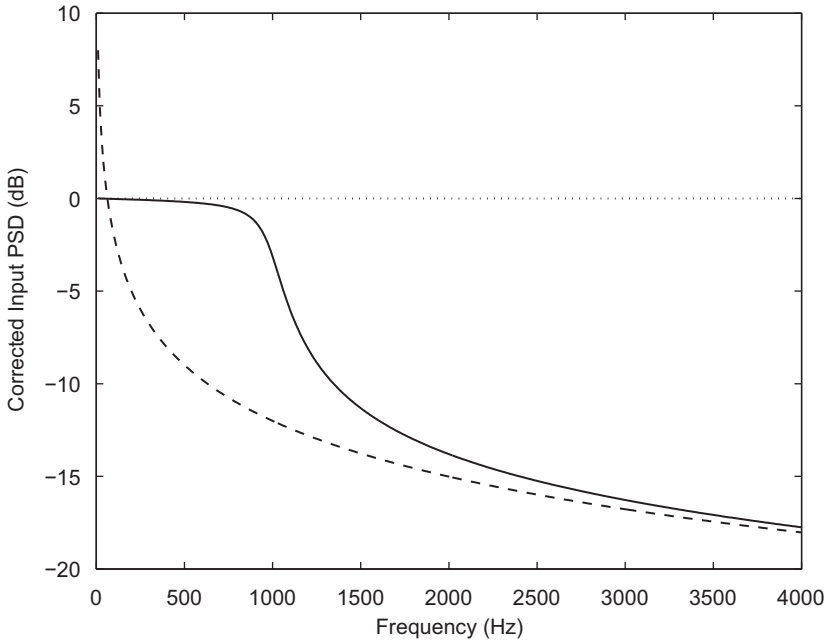

Fig. 9. Corrected input power spectral density functions due to wall pressure fluctuations modeled over the coarse mesh using the filtered power method (solid line) and the uncorrelated model (dashed line).

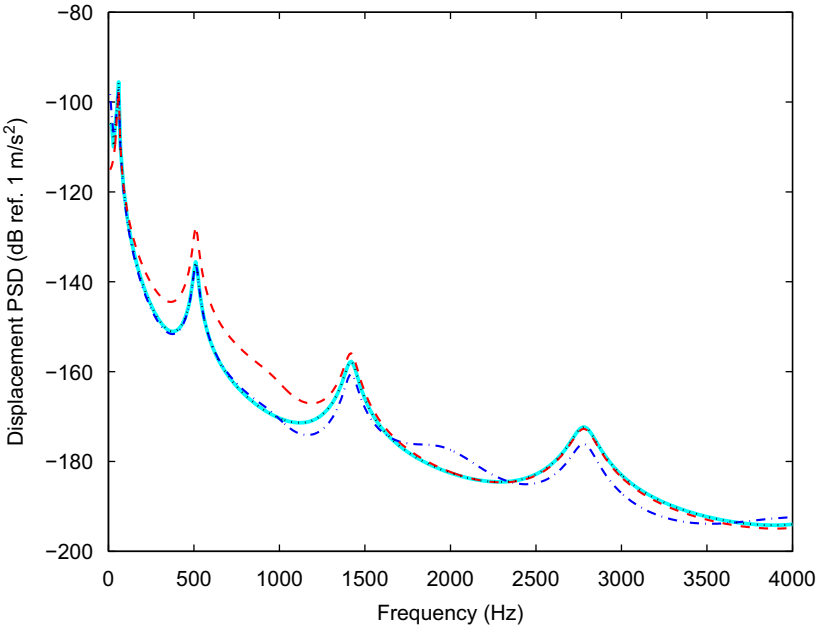

Fig. 10. Comparison of the displacement power spectral density functions at $x=0.5$ m calculated by the correlated filtered power (dash-dotted line), the uncorrelated filtered power (dashed line) and the uncorrelated model (dotted line) with the exact solution (thick solid line) when $U_c=20$ m/s.

To compensate the lost correlation, we can add meshes inside the element. Then, if we add K more nodes,

$$S_{u_j u_j}(\omega)=\sum_{a=1}^{N}\sum_{k=0}^{K}\sum_{l=0}^{K}H_{a_k j}S_{a_k a_l}H^{*}_{a_k j}, \tag{26}$$

where $H_{a_k j}$ is the response function at j to the unit input at the supplementary node k and $S_{a_k a_l}$ is the input PSDF of the forces at the supplementary nodes k and l. Considering that the mesh satisfies the requirement for response representation, the nodal points of the added mesh are very close relative to the wavelength of the response. Hence, $H_{aj}=H_{a_k j}$ for all k's. As a result, Eq. (26) becomes

$$S_{u_j u_j}(\omega)=\sum_{a=1}^{N}|H_a|^2\sum_{k=0}^{K}\sum_{l=0}^{K}S_{a_k a_l}. \tag{27}$$

Rewriting Eq. (27) in the matrix form yields the same equation as Eq. (14) but $\mathbf{S}_{\mathrm{IN}}$ becomes a diagonal matrix. Its diagonal terms are

$$\tilde{S}_{aa}=\sum_{k=0}^{K}\sum_{l=0}^{K}S_{a_k a_l} \tag{28}$$

for each a. This compensation procedure changes the correlated distributed loading into the uncorrelated loadings having the PSDF, given by Eq. (28), over the coarse mesh. Utilizing the Corcos Model for WPF given by Eq. (1), we can explicitly express the uncorrelated loadings at nodes. The WPF can be written in the form of equivalent nodal forces so that, for one-dimensional structures,

$$S_{a_k a_l}(\omega)=\Phi_{a_k a_l}(\gamma_x;\omega)(\Delta x/K)^2, \tag{29}$$

where $\Delta x/K$ represents the effective area at the nodes a_k and a_l. Note that γ_x denotes the relative distance between the nodes a_k and a_l. The PSDF of WPF, $\Phi_{a_k a_l}(\gamma_x;\omega)$, hence, depends on the relative distance. We can then rewrite Eq. (27) with a new index, n, to denote the relative distance as

$$\tilde{S}_{aa}=K\sum_{n=0}^{K}\Phi_{a_k a_l}(n\Delta x/K;\omega)(\Delta x/K)^2, \tag{30}$$

where $n=|l-k|$. Consider an infinite number of added meshes in the element, and so $K\to\infty$. Eq. (30) becomes

$$\tilde{S}_{aa}=\lim_{K\to\infty}\Delta x\sum_{n=0}^{K}\Phi_{a_k a_l}(n\Delta x/K;\omega)(\Delta x/K), \tag{31}$$

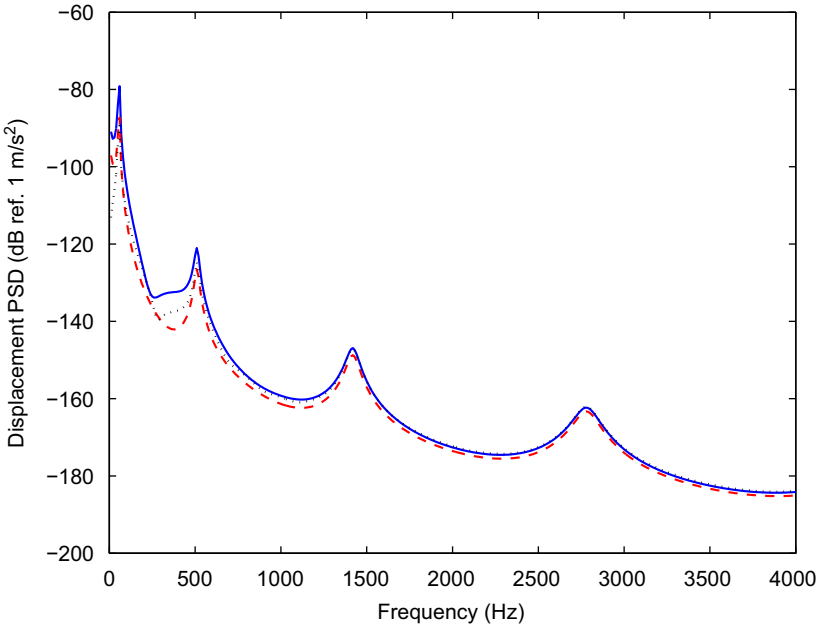

Fig. 11. Comparison of the displacement power spectral density functions at $x = 0.5$ m calculated by the correlated filtered power (solid line) and the uncorrelated model (dashed line) with the exact solution (dotted line) when $U_c = 200$ m/s.

which can be written in the integration form

$$\tilde{S}_{aa} = \Delta x \int_{-\infty}^{-\infty} C_{pq}(\gamma_x; \omega)\, \mathrm{d}\gamma_x. \tag{32}$$

It should be noted that the integration domain should be $-\Delta x \le \gamma_x \le \Delta x$, but it can be, in Eq. (32), $-\infty \le \gamma_x \le \infty$ because the cross-correlation does not exist beyond Δx. Substituting Eq. (1) into (31) and taking the real part, Eq. (32) becomes

$$\tilde{S}_{aa} = \frac{\alpha \Delta x}{\omega / U_c(\alpha^2 + 1)}. \tag{33}$$

The displacement power spectral density function, $S_{u_j u_j}$, can be obtained by utilizing Eq. (27) with Eq. (33) as

$$S_{u_j u_j}(\omega) = \sum_{a=1}^{N} |H_a|^2 \tilde{S}_{aa}. \tag{34}$$

Eq. (34) implies that the WPF can be modeled as uncorrelated loading with the corrected power. The dashed line in Fig. 9 shows the approximate auto-power spectral density function of the WPF.

We again modeled the WPF over the beam structure as the uncorrelated loading given by Eq. (33) for $U_c = 20$ m/s. The maximum mesh size was determined by the requirement for depicting the response given by Eq. (20). The WPF is modeled by the uncorrelated loading with the compensation denoted by the dashed line in Fig. 9. In Fig. 10, the calculated displacement PSDF at $x = 0.5L$ of the beam with the uncorrelated loading given by Eq. (33) (dashed line) is compared with the exact solution (thick solid line). They well agree even at the frequencies where the loading due to the WPF is strongly correlated over the mesh ($2\pi f / U_c < k_{\max}$). Note that this uncorrelated loading scheme (dashed line) gave a solution that is closer to the exact solution than the filtered power scheme (dot-dashed line) demonstrated in Section 3.3.

The excitation due to WPF for $U_c = 200$ m/s was applied to the beam. At this high convective speed, $k_{\max}^{(r)} > k_{\max}^{(e)}$. So, the maximum mesh size determined above using the requirement for depicting the response given by Eq. (20) satisfied the requirement for the excitation modeling automatically. Fig. 11 shows the calculated displacement PSDF at $x = 0.5L$ of the beam with the uncorrelated loading (dashed line) for $U_c = 200$ m/s. It is compared with the exact solution (dotted line), showing good agreement over the frequencies. The smaller correlation length at the higher convective velocity improved the accuracy in the response to the corrected uncorrelated power of WPF.

4. Conclusion

A finite element modeling of the wall pressure fluctuations was investigated in this paper to analyze the dynamic response of structures. A fully correlated loading model, a filtered power model and an uncorrelated model were presented

and they were verified in comparison with an exact solution for a simple beam structure. The main conclusions of this study are as follows.

1. For a fully correlated loading model of WPF, the maximum mesh size should be obtained taking into account the spatial variation of the response as well as the WPF at the highest frequency of interest. The requirement of the mesh size to well depict spatial variation was presented explicitly. To obtain a reliable response at a low frequency, upstream effect should be accounted for by using a dummy mesh outside the structure. Furthermore, very fine meshes are needed to reflect the correlation at high frequencies. This complexity makes finite element modeling difficult in practice. The high correlated power representation because of the dummy structure and the fine mesh leads to the difficulty in modeling. The power, however, did not couple into the modes to be superposed in most cases.
2. Applying the filtered power model of WPF, a reliable structural response can be obtained. To maintain accuracy in the response at low frequencies, the WPF should be modeled with the correlated loading over a coarse mesh that satisfies only the requirement for response representation. When the WPF is modeled as uncorrelated, the response is reliable only at high frequencies such that $2\pi f/U_c < k_{\max}$.
3. An uncorrelated loading model of WPF was proposed. This model was based on the compensation of power which is strongly correlated within the maximum mesh size. Using this scheme of modeling WPF, the structural response can be obtained by simply applying independent random loading at each nodal point.

References

[1] F.M. White, *Fluid Mechanics*, McGraw-Hill Inc., New York, 1979.
[2] W.W. Willmarth, Wall pressure fluctuations in a turbulent boundary layer, *Journal of Acoustical Society of America* 28 (1956) 1048–1053.
[3] R.H. Kraichnan, Pressure fluctuations in turbulent flow over a flat plate, *Journal of Acoustical Society of America* 28 (1956) 378–390.
[4] W.K. Blake, *Mechanics of Flow-Induced Sound and Vibration*, vol. I, Academic Press Inc., 1986.
[5] W.K. Blake, *Mechanics of Flow-Induced Sound and Vibration*, vol. II, Academic Press Inc., New York, 1986.
[6] G.M. Corcos, The structure of the turbulent pressure field in boundary-layer flows, *Journal of Fluid Mechanics* 18 (1964) 335–378.
[7] D.M. Chase, Modeling the wavevector-frequency spectrum of turbulent boundary layer wall pressure, *Journal of Sound and Vibration* 70 (1) (1980) 29–67.
[8] J.E. Ffowcs Williams, Boundary-layer pressures and the Corcos model: a development to incorporate low-wavenumber constraints, *Journal of Fluid Mechanics* 125 (1982) 9–25.
[9] H.S. Ribner, Response of a flexible panel to turbulent flow: running wave versus modal density analysis, *Journal of Acoustical Society of America* 40 (1966) 721–726.
[10] G. Maidanik, Acoustic radiation from a driven infinite plate backed by a parallel infinite baffle, *Journal of Acoustical Society of America* 42 (1967) 27–31.
[11] J. Dyer, Response of plates to a decaying and convecting random pressure field, *Journal of Acoustical Society of America* 31 (1959) 922–928.
[12] P.H. White, Transduction of boundary layer noise by a rectangular panel, *Journal of Acoustical Society of America* 40 (1966) 1354–1362.
[13] L. Maestrello, Use of turbulent model to calculate the vibration and radiation responses of a panel with practical suggestions for reducing sound level, *Journal of Sound and Vibration* 5 (1967) 407–448.
[14] W.A. Strawderman, R.S. Brand, Turbulent-flow-excited vibration of a simply supported rectangular flat plate, *Journal of Acoustical Society of America* 45 (1969) 177–192.
[15] M.L. Rumerman, Frequency-flow speed dependence of structural response to turbulent boundary layer pressure excitation, *Journal of Acoustical Society of America* 91 (2) (1992) 907–910.
[16] K.K. Shin, C. Hong, Vibration analysis of plates subjected to turbulent flows, Technical Report NWSD-513-990395, Agency for Defense Development, 1999.